

Article

Propagation Property of an Astigmatic sin-Gaussian Beam in a Strongly Nonlocal Nonlinear Media

Kaicheng Zhu ¹, Jie Zhu ^{2,*}, Qin Su ² and Huiqin Tang ³

¹ Department of Electronics and Information Engineering, Guangzhou College of Technology and Business, Guangzhou 510850, China; kczhu058@csu.edu.cn

² College of Science, Guizhou Institute of Technology, Guiyang 550003, China; 20140555@git.edu.cn

³ School of Physics and Electronics, Central South University, Changsha 410083, China; gjpcs_16@163.com

* Correspondence: jiezh_16@163.com

Received: 31 October 2018; Accepted: 19 December 2018; Published: 25 December 2018



Abstract: Based on the Snyder and Mitchell model, a closed-form propagation expression of astigmatic sin-Gaussian beams through strongly nonlocal nonlinear media (SNNM) is derived. The evolutions of the intensity distributions and the corresponding wave front dislocations are discussed analytically and numerically. It is generally proved that the light field distribution varies periodically with the propagation distance. Furthermore, it is demonstrated that the astigmatism and edge dislocation nested in the initial sin-Gaussian beams greatly influence the pattern configurations and phase singularities during propagation. In particular, it is found that, when the beam parameters are properly selected, a vortex beam with perfect doughnut-shaped profile can be obtained for astigmatic sin-Gaussian beams with two-lobe pattern propagating in SNNM.

Keywords: nonlocal nonlinear medium; astigmatic sin-Gaussian beam; screw dislocation; edge dislocation; vortex

1. Introduction

In the past decades, self-trapped optical beams in nonlocal nonlinear media, especially in strongly nonlocal nonlinear media (SNNM), have been a topic of considerable interest due to their theoretical importance and many experimental observations [1,2]. SNNM is a novel kind of media in which the characteristic length of the nonlocal response is much larger than the beam width. Distinct from the conventional local nonlinearity, the nonlocality allows the refractive index of the media at a particular point to be related to the beam intensity at all other points. Note that the nonlocal nonlinearity which can support a variety of nonlocal spatial optical solitons exhibits in many physical systems, and some of them have been observed experimentally [3–10]. Moreover, it has been reported that a great number of optical beams can steadily propagate in SNNM under sufficient conditions, including Gaussian beams and higher-order Gaussian beams, four-petal Gaussian beams, Lorentz-Gaussian beams, the beams carrying wave front dislocations such as Hermite-, Hermite-cosh- or Laguerre-Gaussian beams, and so on [11–26]. As well known, pure wave front dislocations in a monochromatic wave are divided into two types: one is the longitudinal screw dislocation which is also known as the optical vortex with spiral phase, and the other is the transverse edge dislocation with π -phase shift located along a line in the transverse plane. During the past years, most of the previous investigations on propagation of beams in SNNM have been focused on those beams whose pattern structure remains invariant although the pattern size may change during propagation. Due to the complexity of evolution of beams in the nonlocal domain, it is interesting to find that the changes of wave front dislocations are possible, which turns out to be very important for the propagation characteristics and will modify the pattern structure for a laser beam in SNNM [24,27,28].

Like Hermite-Gaussian beams, sin-Gaussian beams carrying edge dislocations are the special case of the Hermite-sinusoidal-Gaussian beams whose propagation dynamics through various optical systems had been studied widely [29–37]. However, their propagation in SNNM remains unexplored. In this work, we aim to study the propagation of sin-Gaussian beams with astigmatism in SNNM. A closed-form propagation equation of astigmatic sin-Gaussian beams in SNNM is derived and illustrated with numerical examples. Our results show some novel variations of wave front dislocations occur for astigmatic sin-Gaussian beams propagating in SNNM. The remainder parts of this paper are organized as follows: Section 2 represents the theoretical formulation for astatic sin-Gaussian beams propagating in SNNM. In Section 3 main characters associated with intensity and phase distributions of a propagating sin-Gaussian beam are analytically investigated and a large number of numerical calculations are performed based on the obtained formulae in Section 2. Finally, in Section 4 the main results obtained in this paper are summarized.

2. Theoretical Formulation

In the Cartesian coordinate system, a sin-Gaussian beam with astigmatism in the source plane $z = 0$ takes the form as

$$E(x, y, 0) = \exp \left[-\frac{x^2 + y^2}{w_0^2} - \frac{ik}{2} \left(\frac{x^2}{R_{0x}} + \frac{y^2}{R_{0y}} \right) \right] \sin \left(\frac{\beta_x x + \beta_y y}{w_0} \right) \tag{1}$$

where β_x and β_y represent the parameters associated with the sin part, $k = 2\pi/\lambda$ and λ is the wavelength, w_0 is the spot size of the beam, and R_{0x} and R_{0y} are respectively the curvatures along the x and y directions at $z = 0$. The astigmatism is represented by the curvature difference between x and y directions and can be easily realized in experiment [38,39].

Because the nonlocal nonlinear Schrodinger equation governing the evolution dynamics of optical beams propagating in nonlocal nonlinear medium remains mathematically complicated, in this paper the medium is assumed to be SNNM and, then, Snyder and Mitchell model is appropriate. In fact, it has been found that the analytical solutions obtained from Snyder and Mitchell model and the numerical simulations based on the nonlocal nonlinear Schrodinger equation are in good agreement in the case of strong nonlocality [12,16,18]. The relation between optical beams propagating in SNNM and in quadratic-index media or through optical fractional Fourier transform systems has also been determined [40,41].

The propagation of a sin-Gaussian beam in SNNM is governed by the following equation:

$$2ik \frac{\partial}{\partial z} E(x, y, z) + \left(\frac{\partial^2}{\partial x^2} + \frac{\partial^2}{\partial y^2} \right) E(x, y, z) - k^2 \gamma^2 p_0 (x^2 + y^2) E(x, y, z) = 0 \tag{2}$$

where γ is the material constant relating to the response function, and p_0 is the input power in the source plane. The solution of Equation (2) can be expressed as [15,21,22]

$$E(x, y, z) = \frac{i}{\lambda B} \exp \left[\frac{ikD}{2B} (x^2 + y^2) \right] \iint dx_0 dy_0 E(x_0, y_0, 0) \exp \left[\frac{ikA}{2B} (x_0^2 + y_0^2) - \frac{ik}{B} (xx_0 + yy_0) \right] \tag{3}$$

where the ABCD transfer matrix for SNNM has been obtained with the following:

$$\begin{pmatrix} A & B \\ C & D \end{pmatrix} = \begin{pmatrix} \cos(\pi z_s) & -z_p \sin(\pi z_s) \\ \sin(\pi z_s)/z_p & \cos(\pi z_s) \end{pmatrix} \tag{4}$$

with $z_p = 1/\sqrt{\gamma^2 p_0}$ and $z_s = z/(\pi z_p)$ being the scaled propagation distance.

Substituting Equation (1) into Equation (3) and performing some mathematical manipulations we have

$$E(x, y, z) = \frac{1}{2\lambda B} \exp\left[\frac{iz_R D(x_w^2 + y_w^2)}{B}\right] \iint dx_0 dy_0 \exp\left[-(1 - i\alpha_x) \frac{x_0^2}{w_0^2} - (1 - i\alpha_y) \frac{y_0^2}{w_0^2}\right] \times \left\{ \exp\left[i\left(\beta_x - \frac{2z_R x_w}{B}\right) \frac{x_0}{w_0} + i\left(\beta_y - \frac{2z_R y_w}{B}\right) \frac{y_0}{w_0}\right] - \exp\left[-i\left(\beta_x + \frac{2z_R x_w}{B}\right) \frac{x_0}{w_0} - i\left(\beta_y + \frac{2z_R y_w}{B}\right) \frac{y_0}{w_0}\right] \right\} \tag{5}$$

with

$$\alpha_u = \frac{A k w_0^2}{B} - \frac{k w_0^2}{2R_{0u}} = \frac{Az_R}{B} - \frac{z_R}{R_{0u}} \tag{6}$$

$u_w = u/w_0$ ($u = x$ and y) being scaled transversal coordinates and $z_R = k w_0^2 / 2 = \pi w_0^2 / \lambda$ being the Rayleigh distance. Making use of the Gaussian integral formula

$$\int_{-\infty}^{\infty} \exp(-\alpha x^2 + \beta x) dx = \sqrt{\frac{\pi}{\alpha}} \exp\left(\frac{\beta^2}{4\alpha}\right) \text{Re}(\alpha) > 0 \tag{7}$$

One obtains

$$E(x, y, z) = E_0 \exp\left[-\frac{z_R^2}{B^2} \left(\frac{x_w^2}{1 - i\alpha_x} + \frac{y_w^2}{1 - i\alpha_y}\right)\right] \sinh\left[\frac{z_R}{B} \left(\frac{\beta_x x_w}{1 - i\alpha_x} + \frac{\beta_y y_w}{1 - i\alpha_y}\right)\right] \tag{8}$$

where

$$E_0 = \frac{z_R}{2B\sqrt{(1 - i\alpha_x)(1 - i\alpha_y)}} \exp\left[\frac{iDz_R}{B} (x_w^2 + y_w^2) - \frac{\beta_x^2}{4(1 - i\alpha_x)} - \frac{\beta_y^2}{4(1 - i\alpha_y)}\right] \tag{9}$$

is an axial symmetry factor on a specified observation plane. Equation (8) is the main result obtained in this paper and is also the starting equation to discuss the evolution property of the propagating beam in the next section.

3. Evolutions of Wave Front Dislocations and Intensity Patterns Occurring in an Astigmatic Sin-Gaussian Beam

In this section, we mainly study the evolution of the intensity pattern as well as the wave front dislocation for a sin-Gaussian beam with astigmatism propagating in SNNM using the analytical formulae derived in previous section. According to Equation (8) and the relations of A, B, D, α_x and α_y with the scaled propagation distance z_s , one can generally prove

$$E(x, y, z_s) = E(x, y, z_s + 1) \tag{10}$$

Equation (10) reveals that the evolution of the field distribution with the scaled propagation distance z_s is periodic and the period of the field distribution evolution equals to 1 corresponding to the propagation distance $\pi z_p = \pi z_R \sqrt{p_{Gc}/p_0}$ where $p_{Gc} = 1/(\gamma^2 z_R^2)$ is the critical power of Gaussian or higher-order Gaussian beams. Obviously, $z_p = z_R$ corresponds to $p_0 = p_{Gc}$ while $z_p < z_R$ corresponds to $p_0 > p_{Gc}$.

It is known that a sin-Gaussian beam carries an edge dislocation along the straight line $\beta_x x + \beta_y y = 0$ where β_x and β_y determines the orientation of the edge dislocation and its intensity pattern is a two-lobe configuration for sufficiently small β_x and β_y . For $R_{0x} = R_{0y}$ (i.e., $\alpha_x = \alpha_y$) corresponding to beams without astigmatism, Equation (8) turns to

$$E(x, y, z) = E_0 \exp\left[-\frac{z_R^2 (x_w^2 + y_w^2)}{B^2 (1 - i\alpha_x)}\right] \sinh\left[\frac{z_R (\beta_x x_w + \beta_y y_w)}{B (1 - i\alpha_x)}\right] \tag{11}$$

Regardless of astigmatism, for β_x or β_y being 0, to be specific, assuming $\beta_y = 0$, Equation (8) becomes

$$E(x, y, z) = E_0 \exp \left[-\frac{z_R^2}{B^2} \left(\frac{x_w^2}{1 - i\alpha_x} + \frac{y_w^2}{1 - i\alpha_y} \right) \right] \sinh \left[\frac{z_R \beta_x x_w}{B(1 - i\alpha_x)} \right] \quad (12)$$

Therefore, Equations (11) and (12) clearly demonstrate that the initial edge dislocation remains unchanged for beams without astigmatism propagating in SNNM.

Figure 1 shows typical evolutions of the intensity distributions of sin-Gaussian beams without astigmatism propagating in SNNM at various scaled propagation distance z_s for different values of R_{0x} (R_{0y}) and z_p (z_R) with sufficiently small β_x and β_y . Note that only for $z_p = z_R$ (i.e., $p_0 = p_{Gc}$) and $R_{0x} = R_{0y} = \infty$, sin-Gaussian beam can roughly keep its structure and size unchanged during propagation in SNNM, seeing Row 2 in Figure 1. Otherwise, the pattern size varies with a period of πz_p although the intensity pattern continues to be a two-lobe structure during propagation. This is consistent with those of Gaussian and higher-order Gaussian beams in SNNM [1]. Moreover, the calculations also indicate that the edge dislocation nested in the input sin-Gaussian beam always remains during propagation. However, for sufficiently large values of β_x and β_y , the intensity pattern changes periodically and is independent from the input power p_0 , which can be seen from Figure 2. In the following we only consider the case of small β_x and β_y .

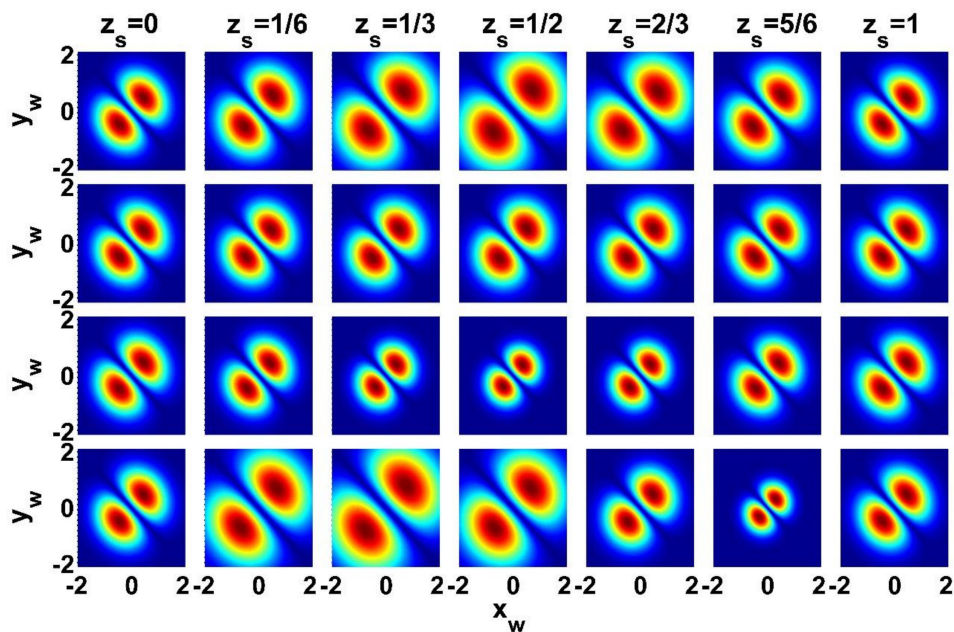


Figure 1. Evolution of intensity distributions of sin-Gaussian beams with the scaled propagation distance z_s for $\beta_x = 0.6, \beta_y = 0.6$. The other parameters are for Row 1: $R_{0x} = R_{0y} = \infty$ and $z_p = \sqrt{2}z_R$; Row 2: $R_{0x} = R_{0y} = \infty$ and $z_p = z_R$; Row 3: $R_{0x} = R_{0y} = \infty$ and $z_p = z_R/\sqrt{2}$ and Row 4: $R_{0x} = R_{0y} = z_R$ and $z_p = z_R$, respectively.

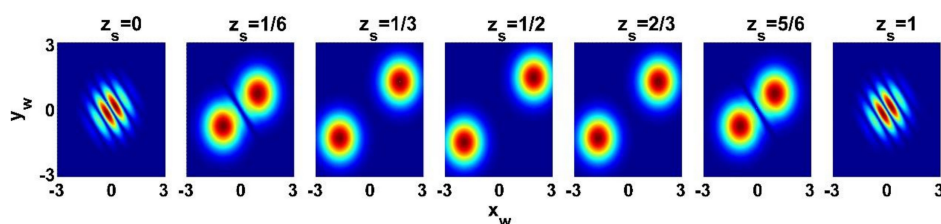


Figure 2. Evolution of intensity distributions of sin-Gaussian beams with the scaled propagation distance z_s for $\beta_x = 4, \beta_y = 3$. The other parameters are $R_{0x} = R_{0y} = \infty$ and $z_p = z_R$.

On the other hand, for $\beta_x \neq 0, \beta_y \neq 0$ and $R_{0x} \neq R_{0y}$ (i.e., $\alpha_x \neq \alpha_y$) corresponding to beams with astigmatism, Equation (8) turns into:

$$E(x, y, z) = E_0 \exp \left[-\frac{z_R^2}{B^2} \left(\frac{x_w^2}{1+\alpha_x^2} + \frac{y_w^2}{1+\alpha_y^2} \right) - \frac{iz_R^2}{B^2} \left(\frac{\alpha_x x_w^2}{1+\alpha_x^2} + \frac{\alpha_y y_w^2}{1+\alpha_y^2} \right) \right] \sinh \left[\frac{z_R}{B} \left(\frac{\beta_x x_w}{1+\alpha_x^2} + \frac{\beta_y y_w}{1+\alpha_y^2} \right) + i \frac{z_R}{B} \left(\frac{\alpha_x \beta_x x_w}{1+\alpha_x^2} + \frac{\alpha_y \beta_y y_w}{1+\alpha_y^2} \right) \right] \tag{13}$$

Since the necessary condition of wave front singularity occurrence is $E(x, y, z) = 0$, it must simultaneously require

$$\frac{\beta_x x_w}{1+\alpha_x^2} + \frac{\beta_y y_w}{1+\alpha_y^2} = 0 \frac{\alpha_x \beta_x x_w}{1+\alpha_x^2} + \frac{\alpha_y \beta_y y_w}{1+\alpha_y^2} = n\pi \quad n = 0, \pm 1, \pm 2, \dots \tag{14}$$

Solving Equation (14) one obtains

$$\frac{\beta_x x_{w,n}}{1+\alpha_x^2} = -\frac{\beta_y y_{w,n}}{1+\alpha_y^2} = \frac{n\pi}{\alpha_x - \alpha_y} \tag{15}$$

These are discrete points at which the intensity is null on the observation plane. Especially, $n = 0$ corresponds to a solitary zero intensity point at $(x_w, y_w) = (0, 0)$. This implies that, due to the simultaneous existence of an edge dislocation and astigmatism in an input beam, the wave front dislocation structure varies and the zero-intensity line of an input edge dislocation can evolve into some discrete null intensity points during propagation. Obviously, an astigmatism ($R_{0x} \neq R_{0y}$) as well as the orientation of the initial edge dislocation determined by β_x (β_y) are very key factors for the variation of wave front dislocation embedded in a propagating sin-Gaussian beam.

Based on the analytical discussions previously mentioned, a large number of numerical calculations are performed and typical numerical examples are chosen to illustrate the general propagation features for the astigmatic sin-Gaussian beam in SNNM. For the case of $R_{0x}R_{0y} > 0$ or R_{0x} and R_{0y} having the same sign as shown in Figure 3, the input astigmatic sin-Gaussian beam is a two-lobe pattern only carrying an edge dislocation. Such propagating beam evolves into one with a dark-hollow pattern and a screw dislocation (vortex) because the lines of zero real- and imaginary-part associated with the propagating field distribution intersect at the origin. It can be seen that the pattern configuration changes with period πz_p during propagation, and so do the phase singularities varying between an edge-dislocation and a screw dislocation.

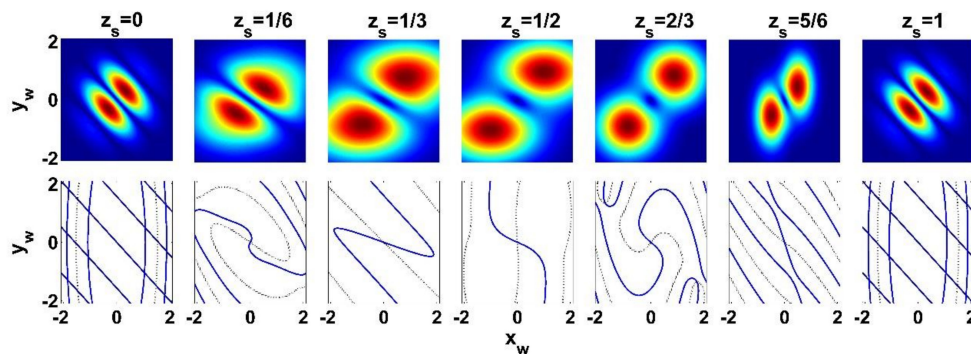


Figure 3. Evolution of field distributions of a sin-Gaussian beam with the scaled propagation distance z_s for $z_p = z_R, \beta_x = \beta_y = 2, R_{0x} = 3z_R/4, R_{0y} = 10z_R$. Upper row: Intensity distribution $|E(x, y, z)|^2$; Bottom row: $\text{Re}\{E(x, y, z)\} = 0$ (solid lines) and $\text{Im}\{E(x, y, z)\} = 0$ (dashed lines), respectively.

When the signs of R_{0x} and R_{0y} are different or one of them is ∞ , the input sin-Gaussian beam carries a mixed dislocation consisting of a vortex and an edge dislocation at the origin because there is an intersection point at $(0,0)$ of both the straight lines $\beta_x x + \beta_y y = 0$ and $\frac{x^2}{|R_{0x}|} - \frac{y^2}{|R_{0y}|} = 0$ which

respectively relate to the zero real- and imaginary-part of the input beam. Figure 4 shows a typical example for $\beta_x = \beta_y = 1/3$, $R_{0x} = 3z_R/4$ and $R_{0y} = \infty$, revealing that the mixed dislocations in the source plane turns into a vortex with period πz_p during propagation. The calculations further confirm that the size of the patterns also depends on the values of the input power p_0 .

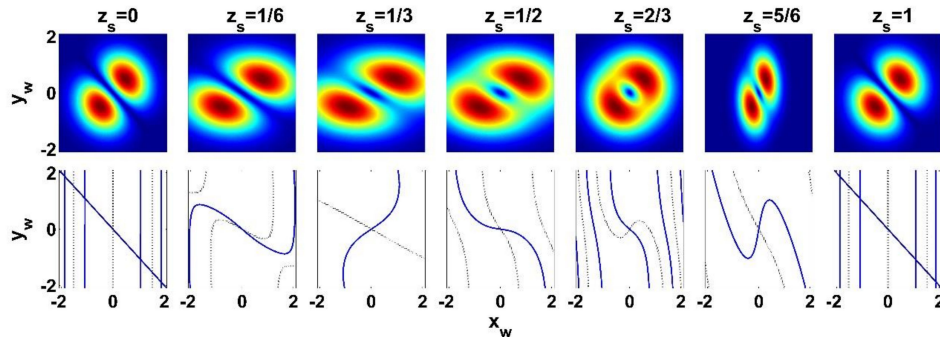


Figure 4. Same as Figure 3 but for $z_p = z_R$, $\beta_x = \beta_y = 1/3$, $R_{0x} = 3z_R/4$, $R_{0y} = \infty$.

For specified choices of $R_{0x} = -R_{0y}$ and smaller values of $\beta_x = \pm \beta_y$, interestingly, it can be observed that an astigmatic sin-Gaussian beam evolves into a doughnut-shaped pattern with a uniform bright enclosure. Figures 5 and 6 show evolutions of the intensity distributions of astigmatic sin-Gaussian beams in SNNM for different values of z_p with $R_{0x} = -R_{0y} = z_R$, $\beta_x = \beta_y = 1/3$. Obviously, the propagating beam forms a perfect doughnut-shaped pattern across the transverse plane at $z_s = 1/2$. Note that the size of the preferred doughnut-shaped pattern at $z_s = 1/2$ sensitively depends on the values of the parameter z_p , or to be more specific, the size of the doughnut-shaped pattern decreases with an increase of the input power p_0 . Moreover, we also investigate the wave front dislocation evolutions of the propagation field, demonstrating that the canonical vortex is invariant for $z_p = z_R$ but evolves into noncanonical for other values of z_p , which can be seen from these figures.

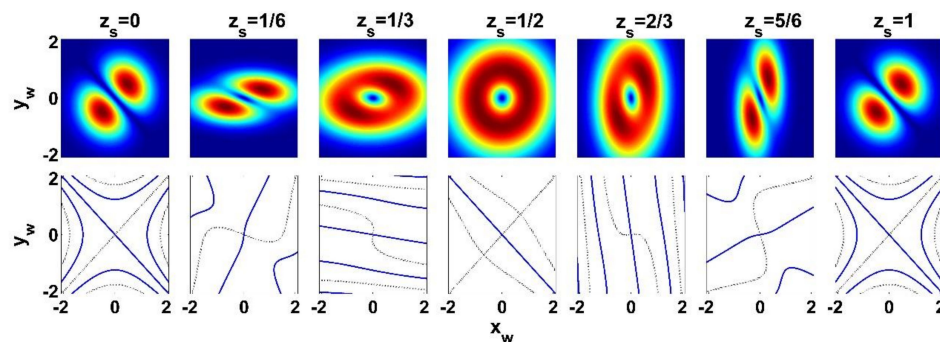


Figure 5. Same as Figure 4 but for $\beta_x = \beta_y = 1/3$, $z_p = R_{0x} = -R_{0y} = z_R$.

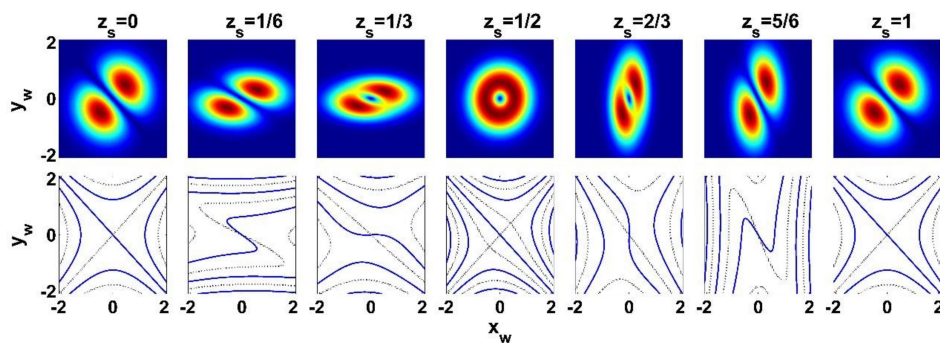


Figure 6. Same as Figure 5 but for $z_p = z_R/\sqrt{3}$.

In fact, for the specified choice $R_{0x} = -R_{0y} = z_R$, $z_s = 1/2$ and $\beta_x = \pm\beta_y = \beta$, we have $\alpha_{x,y} = \pm 1$, $A = 0$, $B = -z_p$. With the cylindrical coordinates $x_w = r\cos\theta$ and $y_w = r\sin\theta$, Equation (8) transforms to:

$$E(r, \theta, z) = E_0 \exp\left[-\frac{z_R^2 r^2 (1 - i \cos 2\theta)}{2z_p^2}\right] \sinh\left(\frac{z_R \beta}{\sqrt{2}z_p} r e^{\pm i(\theta + \pi/4)}\right) \quad (16)$$

For sufficiently small $\frac{z_R \beta}{\sqrt{2}z_p}$, Equation (16) can approximate to:

$$E(r, \theta, z) \approx E_0 \frac{z_R \beta}{\sqrt{2}z_p} \exp\left(-\frac{z_R^2 r^2}{2z_p^2}\right) r e^{\pm i(\theta + \pi/4)} \quad (17)$$

which just represents a vortex beam and agrees with the numerical results.

Finally, it should be pointed out that, for $\lambda = 500$ nm and $w_0 = 1$ mm, one has $z_R \approx 6.28$ m and the curvatures R_{0x} and R_{0y} approximate to z_R , which is realizable in experiment. When the sin-Gaussian beam is produced with a sine-amplitude modulated grating, $|\beta_x| = |\beta_y| < 1/3$ implies that the spatial frequency of the sine-amplitude modulated grating should be below 0.05 lp/mm and is ultra-low, which seems to be a challenging task in manufacturing technology nowadays.

4. Conclusions

In summary, the propagation of astigmatic sin-Gaussian beams in SNNM is investigated in detail. Based on the Snyder and Mitchell model, a closed-form propagation expression of astigmatic sin-Gaussian beams in SNNM is derived. The effect of astigmatism embedded in the input sin-Gaussian beams on the propagation properties is discussed analytically and numerically. It generally proves that the evolution of the field distribution with the propagation distance is periodic. For small values of β_x (β_y), a sin-Gaussian beam with or without astigmatism propagating in SNNM may retain a two-lobe pattern, or transform into a dark hollow pattern and even into a preferred doughnut-shaped profile depending on other parameter choices. Similarly, the phase singularity nested on the input sin-Gaussian beam can maintain its initial dislocation, or change from an edge dislocation to a vortex and even from canonical vortex to a noncanonical one periodically. In particular, theoretical analysis and the numerical simulative results demonstrate that astigmatism and the transversal orientation of the edge dislocation line of the initial sin-Gaussian beam play a key role in realizing these novel transformations during propagation in SNNM. It has been shown theoretically and experimentally that the nematic liquid crystals and the lead glasses are the SNNMs [42–44]. Therefore, the results presented here is intriguing for it reveals that the propagating astigmatic sin-Gaussian beam can transform between a two-lobe pattern and doughnut-shaped pattern in SNNM and furnishes an additional way to realize a doughnut-shaped beam with vortex using a sin-Gaussian beam with edge dislocations.

Author Contributions: Conceptualization, K.Z. and J.Z.; formal analysis, K.Z. and J.Z.; funding acquisition, J.Z.; software, Q.S. and H.T.; supervision, K.Z.; writing—original draft, K.Z. and Q.S.; writing—review and editing, J.Z. and H.T.

Acknowledgments: This research is supported by the high level introduction of talent research start-up fund of Guizhou Institute of Technology, China. Many thanks to the anonymous reviewers for their good suggestions.

Conflicts of Interest: The authors declare no conflict of interest.

References

1. Snyder, A.W.; Mitchell, D.J. Accessible solitons. *Science* **1997**, *276*, 1538–1541. [[CrossRef](#)]
2. Peccianti, M.; Conti, C.; Assanto, G.; De Luca, A.; Umetsu, C. All Optical Switching and Logic Gating with Spatial Solitons in Liquid Crystals. *Appl. Phys. Lett.* **2002**, *81*, 3335–3337. [[CrossRef](#)]

3. Briedis, D.; Petersen, D.E.; Edmundson, D.; Krolkowski, W.; Bang, O. Ring vortex solitons in nonlocal nonlinear media. *Opt. Express* **2005**, *13*, 435–443. [[CrossRef](#)]
4. Lu, D.Q.; Hu, W. Multiringed breathers and rotating breathers in strongly nonlocal nonlinear media under the off-waist incident condition. *Phys. Rev. A* **2009**, *79*, 043833. [[CrossRef](#)]
5. Deng, D.M.; Guo, Q.; Hu, W. Complex-variable-function Gaussian solitons. *Opt. Lett.* **2009**, *34*, 43–45. [[CrossRef](#)]
6. Zhang, S.W.; Yin, L. Two-dimensional Hermite–Gaussian solitons in strongly nonlocal nonlinear medium with rectangular boundaries. *Opt. Commun.* **2009**, *282*, 1654–1658. [[CrossRef](#)]
7. Yang, Z.J.; Ma, X.K.; Zheng, Y.Z.; Gao, X.H.; Lu, D.Q.; Hu, W. Dipole solitons in nonlinear media with an exponential-decay nonlocal response. *Chin. Phys. Lett.* **2011**, *28*, 074213. [[CrossRef](#)]
8. Ge, L.J.; Wang, Q.; Shen, M.; Shi, J.L. Dipole solitons in nonlocal nonlinear media with anisotropy. *Opt. Commun.* **2011**, *284*, 2351–2356. [[CrossRef](#)]
9. Bai, Z.Y.; Deng, D.M.; Guo, Q. Elegant Ince Gaussian breathers in strongly nonlocal nonlinear media. *Chin. Phys. B* **2012**, *21*, 064218. [[CrossRef](#)]
10. Wang, Q.; Li, J.Z. Hermite-Gaussian Vector soliton in strong nonlocal media. *Opt. Commun.* **2014**, *333*, 253–260. [[CrossRef](#)]
11. Lopez-Aguayo, S.; Gutierrez-Vega, J.C. Elliptically modulated self-trapped singular beams in nonlocal nonlinear media: ellipticons. *Opt. Express* **2007**, *15*, 18326–18338. [[CrossRef](#)] [[PubMed](#)]
12. Deng, D.M.; Guo, Q. Propagation of Laguerre-Gaussian beams in nonlocal nonlinear media. *J. Opt. A Pure Appl. Opt.* **2007**, *9*, 0351. [[CrossRef](#)]
13. Yang, Z.J.; Lu, D.Q.; Deng, D.M.; Li, S.H.; Hu, W.; Guo, Q. Propagation of four-petal Gaussian beams in strongly nonlocal nonlinear media. *Opt. Commun.* **2010**, *283*, 595–603. [[CrossRef](#)]
14. Yang, Z.J.; Lu, D.Q.; Hu, W.; Zheng, Y.Z.; Gao, X.H. Hollow Gaussian beams in strongly nonlocal nonlinear media. *Chin. Phys. B* **2010**, *19*, 124212. [[CrossRef](#)]
15. Yang, Z.J.; Lu, D.Q.; Hu, W.; Zheng, Y.Z.; Gao, X.H.; Guo, Q. Propagation of optical beams in strongly nonlocal nonlinear media. *Phys. Lett. A* **2010**, *374*, 4007–4013. [[CrossRef](#)]
16. Deng, D.M.; Guo, Q. Propagation of Cartesian beams in nonlocal nonlinear media. *Eur. Phys. J. D* **2010**, *60*, 355–359. [[CrossRef](#)]
17. Mishra, M.; Hong, W.P. Investigation on propagation characteristics of super-Gaussian beam in highly nonlocal medium. *Prog. Electromagn. Res. B* **2011**, *31*, 175–188. [[CrossRef](#)]
18. Deng, D.M. Propagation of rotating parabolic cylindrical beams in nonlocal nonlinear medium. *Opt. Commun.* **2012**, *285*, 3976–3981. [[CrossRef](#)]
19. Deng, D.; Li, H. Propagation properties of Airy–Gaussian beams. *Appl. Phys. B* **2012**, *106*, 677–681. [[CrossRef](#)]
20. Guan, Y.; Zhong, L.X.; Chew, K.H.; Chen, H.; Wu, Q.Y.; Chen, R.P. Evolution of cos-Gaussian beams in a strongly nonlocal nonlinear medium. *Prog. Electromagn. Res.* **2013**, *141*, 403–414. [[CrossRef](#)]
21. Honarasa, G.; Keshavarz, A. Propagation of the two-dimensional elegant Hermite-cosh-Gaussian beams in strongly nonlocal nonlinear media. *Optik* **2013**, *124*, 6535–6538. [[CrossRef](#)]
22. Zhou, G.Q. Propagation property of a Lorentz–Gauss vortex beam in a strongly nonlocal nonlinear media. *Opt. Commun.* **2014**, *330*, 106–112. [[CrossRef](#)]
23. Zhou, G.Q.; Chen, R.P.; Ru, G.Y. Propagation of an Airy beam in a strongly nonlocal nonlinear media. *Laser Phys. Lett.* **2014**, *11*, 105001. [[CrossRef](#)]
24. Dai, Z.P.; Yang, Z.J.; Zhang, S.M.; Pang, Z.G. Propagation of anomalous vortex beams in strongly nonlocal nonlinear media. *Opt. Commun.* **2015**, *350*, 19–27. [[CrossRef](#)]
25. Zhu, W.; Guan, J.; Deng, F.; Deng, D.M.; Huang, J.W. The propagation properties of the first-order and the second-order Airy vortex beams through strongly nonlocal nonlinear medium. *Opt. Commun.* **2016**, *380*, 434–441. [[CrossRef](#)]
26. Zhang, X.P. Conversion of the high-mode solitons in strongly nonlocal nonlinear media. *J. Mod. Opt.* **2017**, *64*, 170–176. [[CrossRef](#)]
27. Guo, Q.; Luo, B.; Yi, F.; Chi, S.; Xie, Y. Large phase shift of nonlocal optical spatial solitons. *Phys. Rev. E* **2004**, *69*, 016602. [[CrossRef](#)] [[PubMed](#)]
28. Nie, H.X.; Zhang, H.F.; Li, L. Propagation and interaction of beams with initial phase-front curvature in highly nonlocal media. *Opt. Commun.* **2008**, *281*, 5429–5438. [[CrossRef](#)]

29. Casperson, L.W.; Hall, D.G.; Tovar, A.A. Sinusoidal-Gaussian beams in complex optical systems. *J. Opt. Soc. Am. A* **1997**, *14*, 3341–3348. [[CrossRef](#)]
30. Casperson, L.W.; Tovar, A.A. Hermite-sinusoidal-Gaussian beams in complex optical systems. *J. Opt. Soc. Am. A* **1998**, *15*, 954–961. [[CrossRef](#)]
31. Eyyuboglu, H.T.; Baykal, Y. Hermite-sine-Gaussian and Hermite-sinh-Gaussian laser beams in turbulent atmosphere. *J. Opt. Soc. Am. A* **2005**, *22*, 2709–2718. [[CrossRef](#)]
32. Chen, R.P.; Zheng, H.P.; Chu, X.X. Propagation properties of a sinh-Gaussian beam in a Kerr medium. *Appl. Phys. B* **2011**, *102*, 695–698. [[CrossRef](#)]
33. Baykal, Y. Sinusoidal Gaussian beam field correlations. *J. Opt.* **2012**, *14*, 075707. [[CrossRef](#)]
34. Sun, Q.G.; Zhou, K.Y.; Fang, G.Y.; Zhang, G.Q.; Liu, Z.J.; Liu, S.T. Hollow sinh-Gaussian beams and their paraxial properties. *Opt. Express* **2012**, *20*, 9682–9691. [[CrossRef](#)] [[PubMed](#)]
35. Tang, H.Q.; Zhu, K.C. Generation of dark hollow beam by focusing a sine-Gaussian beam using a cylindrical lens and a focusing lens. *Opt. & Laser Technology* **2013**, *54*, 68–71.
36. Zhu, K.C.; Tang, H.Q.; Tang, Y.; Xia, H. Gyrator transform of generalized sine-Gaussian beams and conversion an edge-dislocation into a vortex. *Opt. & Laser Technol.* **2014**, *64*, 11–16.
37. Zhu, J.; Zhu, K.C.; Tang, H.Q.; Xia, H. Average intensity and spreading of an astigmatic sinh-Gaussian beam with small beam width propagating in atmospheric turbulence. *Journal of Modern Optics* **2017**, *64*, 1915–1921. [[CrossRef](#)]
38. Zhu, J.; Zhu, K.C.; Li, X.L.; Su, Q.; Tang, H.Q. Gyrator transform of phase-flipped Gaussian beams and conversion of an edge-dislocation into a vortex. *Optik* **2018**, *156*, 684–688. [[CrossRef](#)]
39. Serna, J.; Nemels, G. Decoupling of coherent Gaussian beams with general astigmatism. *Opt. Lett.* **1994**, *18*, 1774–1776. [[CrossRef](#)]
40. Lu, D.Q.; Hu, W.; Zheng, Y.J.; Liang, Y.B.; Cao, L.G.; Lan, S.; Guo, Q. Self-induced fractional Fourier transform and revivable higher-order spatial solitons in strongly nonlocal nonlinear media. *Phys. Rev. A* **2008**, *78*, 043815. [[CrossRef](#)]
41. Lu, D.Q.; Guo, Q. The relation between optical beam propagation in free space and in strongly nonlocal nonlinear media. *Europhys. Lett.* **2009**, *86*, 44004. [[CrossRef](#)]
42. Conti, C.; Peccianti, M.; Assanto, G. Route to nonlocality and observation of accessible solitons. *Phys. Rev. Lett.* **2003**, *91*, 073901. [[CrossRef](#)] [[PubMed](#)]
43. Conti, C.; Peccianti, M.; Assanto, G. Observation of optical spatial solitons in a highly nonlocal Medium. *Phys. Rev. Lett.* **2004**, *92*, 113902. [[CrossRef](#)] [[PubMed](#)]
44. Rotschild, C.; Cohen, O.; Manela, O.; Segev, M.; Carmon, T. Solitons in nonlinear medium with an infinite range of nonlocality: first observation of coherent elliptic solitons and of vortex-ring solitons. *Phys. Rev. Lett.* **2005**, *95*, 213904. [[CrossRef](#)] [[PubMed](#)]

